IEEE Access
Multidisciplinary | Rapid Review | Open Access Journal

Received January 7, 2020, accepted March 4, 2020, date of publication March 9, 2020, date of current version March 18, 2020.

Digital Object Identifier 10.1109/ACCESS.2020.2979257

Analysis of Hinge's Hysteresis Based on Response Surface Method

MINGXING GAO, HONGWEI GUO, RONGQIANG LIU, AND ZONGQUAN DENG
State Key Laboratory of Robotics and System, Harbin Institute of Technology, Harbin 150001, China

Corresponding authors: Hongwei Guo (guohw@hit.edu.cn) and Rongqiang Liu (liurq@hit.edu.cn)

This work was supported in part by the National Natural Science Foundation of China under Grant 51575119 and Grant 51675114.

ABSTRACT The hinge, a key component of deployable space mechanism, has a significant influence on the precision of the whole mechanism. Hysteresis is one of the uncontrollable factors affecting the precision of the hinge. However, much work so far has focused on the equivalent model of hysteresis, which is far from the actual situation. In this paper, the hysteresis model of the general rotary hinge was established via the finite element method (ABAQUS/Standard 6.14-4). The correctness of the model was verified by experiments, and the loss factor was defined to measure the size of hysteresis. The response surface method was then used to establish the response surface of the hysteresis loss factor of the general rotary hinge. Results show that the hinge was optimised. By comparing the response surfaces of the two types of hinges, the modified hinge can effectively reduce hysteresis loss factor. Importantly, the repeatability of the hinge can be effectively improved by reducing hysteresis loss factor through repeatability experiments. Using this method, the response surface of the hinge's hysteresis loss factor can be established accurately, and the hysteresis loss factor can be reduced through optimal design to improve the precision of the hinge. This method can provide reference and guidance for the hinge design of the high-precision deployable mechanism.

INDEX TERMS Finite element method, hinge, hysteresis, response surface method.

I. INTRODUCTION

With the rapid development of space science and technology, increasingly large in-orbit platforms are applied, and space deployable mechanisms are developed and applied rapidly. For high-precision space deployable mechanism, especially for the supporting mechanism of the large space telescope, having very high space dimensional stability is necessary. The main factors that affect dimensional stability are fabrication, mechanical and kinematic errors. Fabrication errors can be corrected on the ground before launch or corrected by quasi-static on-orbit adjustment. Mechanical errors, arising from the structure's response to dynamic, static and thermal loads, can be corrected via active control. Kinematic errors are mainly caused by the clearance in joints and the hinges' hysteresis. Due to the probability and randomness, the kinematic errors of the mechanism are uncontrollable. Thus, space deployable precision mechanisms should be designed to eliminate the kinematic errors and minimise the influence of mechanical and fabrication errors. For kinematic errors, the clearance can be eliminated by interference fit, preloaded bearings and painting epoxy, whereas the hinges' hysteresis is difficult to control or eliminate generally. NASA Langley Research Center [1]–[3] designed a revolute joint with less than 2% hysteresis to achieve micron-precision deployment requirements in 1996. Lake and Hachkowski [4], [5] introduced the design principles for optical precision deployable mechanism and the guidelines for reducing hysteresis. However, most of them were based on experience summary lacking theoretical analysis. Hassani *et al.* performed a survey of various mathematical models for hysteresis [6]. For the hinges' hysteresis, Bullock [7], [8] adopted the Force–State Mapping method to establish the models of joint's extensional and rotational behaviours and found that the joint's rotational behaviour can be described by Dahl hysteresis loops. Warren and Peterson [9] used unique experimental techniques to measure the repeatability of a precision deployable mechanism at a micron level of resolution. Hinkle [10] studied the frictional microslip through experiments at the nanometer scale and built a theoretical model derived from the constitutive elasticity and roughness. Hachkowski [11] proposed reducing hysteresis through load path management. Hardaway [12] found that permanent hysteresis persists at nanometres of deformation and can be reduced by

The associate editor coordinating the review of this manuscript and approving it for publication was Feiqi Deng.

lower load ratios generally. Heald [13] studied the deployment repeatability of jointed precision structures through examining the sensitivity of the mechanical uncertainty and found that bounding the displacement was possible by using the width of the hysteresis. Footdale [14] designed and developed a multi-axis real-time hybrid measurement platform for precision aerospace structures. Jeon [15] analysed the characterisation of rolling microslip for precision revolute hinge based on the influence function method and stated the optimal improvements for the design of precision hinge. Mann [16] established the equivalent model of precision joint and analysed quasi-static and dynamic responses. The model was also applied to a planar truss. Stohlman [17] analysed the repeatability of ADAM mast considering the cable preload, latch behaviour and hysteresis of joint. Worden and Manson [18], [19] considered the differential evolution as an evolutionary algorithm and adopted the Bouc–Wen model to identify hysteretic systems. Ruderman and Bertram [20] introduced the models and observations of the hysteresis lost motion in elastic robot joints. Swevers *et al.* [21] established a new dynamical friction model, considering the hysteretic behaviour in presliding. Although the hysteresis was studied earlier, the studies were mostly based on the equivalent model, lacking experimental verification, and far from the actual situation. In this work, ABAQUS/Standard 6.14-4 software was employed to analyse contact deformation. The model of hysteresis was established accurately by combining the finite element method (FEM) with experimental verification. The response surface method (RSM) [22]–[24] was used to establish the response surface of the hysteresis loss factor to analyse the influence of various factors on the size of hysteresis.

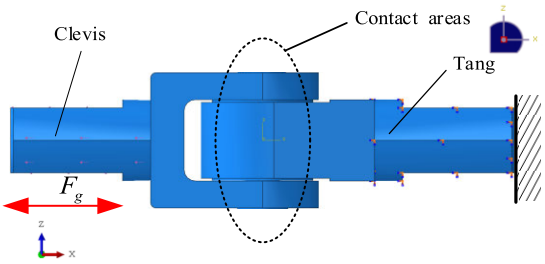

FIGURE 1. FEM of hysteresis for general rotary hinge.

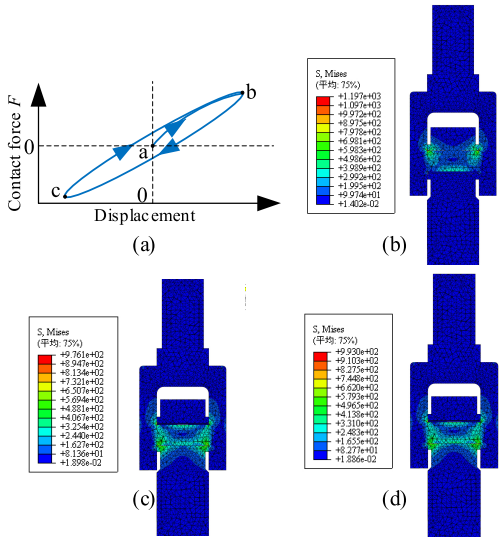

FIGURE 2. Hysteretic motion of the general rotary hinge. (a) Motion diagram. (b) Stretching motion, point a to b. (c) Compression motion, point b to c. (d) Stretching motion, point c to a.

II. HYSTERESIS MODEL OF GENERAL ROTARY HINGE

A. FINITE ELEMENT MODEL OF HYSTERESIS

Fig. 1 shows that the finite element model of the general rotary hinge was established in finite element software ABAQUS. The tang and clevis of the hinge were made of aluminium alloy with Young's Modulus of 71 GPa and Poisson's Ratio of 0.33. The material of the shaft was 45 steel with Young's Modulus of 210 GPa and Poisson's Ratio of 0.31. When defining the contact surface, the contact parts of the tang and clevis were defined as the master surfaces. The contact parts of the shaft were defined as the slave surfaces. The hexahedral reduced integration element (C3D8R) was used to divide the mesh, and the mesh size of the slave surfaces was smaller than the master surface. The tang was fixed, and reciprocating force was applied to the clevis. The amplitude of force was F_g. Furthermore, to improve the convergence of the solution, a tiny contact step was defined before the contact analysis to make contact with contact surfaces. Thus, the relation between contact displacement and contact force of the hinge can be analysed.

Fig. 2 indicates that the hysteretic motion of the hinge consists of the following stages: the forward stretching motion from point a to point b, the backward compression motion from point b to point c, and the forward stretching motion from point c to point b. The hysteresis curve of the general rotary hinge can be obtained by the contact force and displacement curves of the three stages.

The hysteresis loop of the general rotary hinge is shown in Figure 3. The three displacement force curves do not

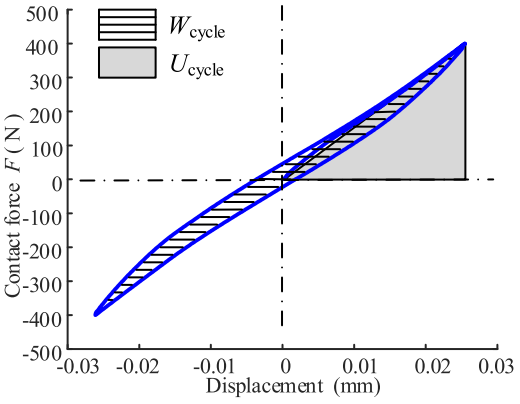

FIGURE 3. Hysteresis loop of the general rotary hinge.

overlap but form an annular force-displacement curve when reciprocating tension and compression are applied to the hinge, that is, the hysteresis loop.

The loss factor η was defined to measure the size of the hysteresis. Specifically, the smaller the η is, the less obvious the hysteresis of the hinge and the higher repeatability will be. The loss factor η was defined as follows:

$$\eta = \frac{W_{\text{cycle}}}{2\pi U_{\max}} \tag{1}$$

where W_{cycle} was the energy dissipated over the hysteretic motion, i.e. the area of the hysteresis loop; and $U_{\max}$ was the maximum strain energy stored per cycle, i.e. the area of the triangle in Fig. 3.

B. MODEL TEST VERIFICATION

To verify the correctness and accuracy of the finite element model, Fig. 4 shows that an experimental measurement platform for hysteresis of hinges was built. The INSTRON 5669 universal testing machine was selected to fully simulate the boundary and load conditions of the finite element model. The tang was fixed, and reciprocating force was applied to the clevis of the hinge. Specifically, stretch the clevis forward to the rated force F_g then compress the clevis to force F_g in the reverse direction. Finally, stretch the clevis to force F_g. The three processes were performed at the same speed of 0.2 mm/min.

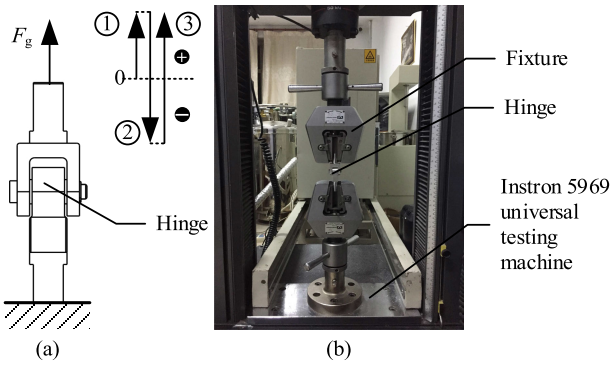

FIGURE 4. Experimental measurement platform of hysteresis for general rotary hinge. (a) Schematic diagram. (b) Experiment device.

The comparison between the test measurement data and the finite element simulation data is shown in Fig. 5. Thus, the test measurement curve and the simulation curve are identical in shape. In particular, under the maximum contact load 400 N, the contact displacement obtained by simulation was 0.0308 mm, and the contact displacement measured by the test was 0.032 mm. The error was 3.77%. Also, by calculating, the loss factor of hinge obtained by finite element simulation was 0.0891. The loss factor measured by the test was 0.0933, with an error of 4.50%. The errors of contact displacement and loss factor are within 5%, and the simulation curve is consistent with the experimental curve. Hence, the finite element simulation model is considered correct and

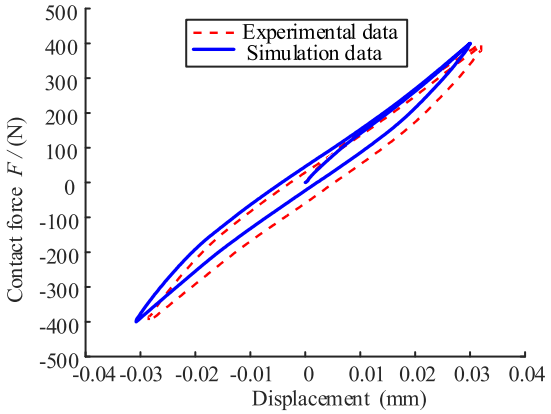

FIGURE 5. Hysteresis test verification of the general rotary hinge.

can be used as a method to study the hysteresis of the general rotary hinge.

III. MATHEMATICAL AGENT MODEL OF HYSTERESIS

A. RSM

The FEM has low solving efficiency and is easy to have nonconvergence problems when solving the contact problem of a hinge. It is difficult to establish with the exact relationships between the hysteresis loss factor and related parameters of the hinge. The polynomial response surface method is to construct the functional expression of the target value based on the response value of the existing design sample points by using empirical formula or numerical analysis. From calculus, any function can be approximated by a polynomial in sections. The polynomial response surface approximation method is a widely used method to obtain the agent model. Its approximate polynomial expression is as follows:

$$\tilde{y}(x) = \sum_{i=1}^{n} \beta_i \varphi_i(x) \tag{2}$$

where $\tilde{y}(x)$ is the response surface value of loss factor of the general rotary hinge; n is the number of polynomials $\varphi_i(x)$; i is the number of independent variables; and β_i is the coefficient of basis function.

The RSM was used to analyse the hysteresis loss factor of the general rotary hinge. Initially, appropriate sample points were selected by the appropriate experimental design method. Subsequently, the sample points were calculated via finite element simulation. Eventually, the proxy model was established by a polynomial. For general rotary hinge, clearance Δr and force amplitude F_g were selected as variables. In addition, the variation ranges were 0–0.4 mm and 100–500 N, respectively. Twenty-five experimental sample points were obtained as listed in Table 1. Higher degree polynomials require more simulation sample points, whereas lower degree polynomials cannot provide sufficient calculation accuracy. The most commonly used polynomial is the fourth-degree polynomial, whose approximate expression is

TABLE 1. Simulation data of hysteresis loss factor for the general rotary hinge.

Num.	Δr/mm	F_g/N	η
1	0	100	0.0656
2	0	200	0.109
3	0	300	0.0997
4	0	400	0.0895
5	0	500	0.0849
6	0.1	100	0.0554
7	0.1	200	0.0989
8	0.1	300	0.0918
9	0.1	400	0.0811
10	0.1	500	0.0759
11	0.2	100	0.0466
12	0.2	200	0.0901
13	0.2	300	0.0841
14	0.2	400	0.0731
15	0.2	500	0.0674
16	0.3	100	0.0401
17	0.3	200	0.0831
18	0.3	300	0.0775
19	0.3	400	0.0658
20	0.3	500	0.0608
21	0.4	100	0.0354
22	0.4	200	0.0769
23	0.4	300	0.0712
24	0.4	400	0.0596
25	0.4	500	0.0555

as follows:

$$\begin{aligned}&1, x_1, x_2 \ldots x_n,\\ &x_1^2, x_1x_2, \ldots, x_1x_n, \ldots, x_n^2,\\ &x_1^3, x_1^2x_2, \ldots, x_1^2x_n, x_1x_2^2, \ldots, x_1x_n^2, \ldots, x_n^3\\ &x_1^4, x_1^3x_2, \ldots, x_1x_n^3, x_1^2x_2^2, \ldots, x_1^2x_n^2, \ldots, x_1\\ &x_2^3, \ldots, x_1x_n^3, \ldots, x_n^4\end{aligned} \tag{3}$$

The polynomial proxy model contains cross terms to ensure high computational accuracy, and the polynomial coefficient can be obtained by the least-square method.

$$b = \left(\mathbf{\Phi}^{\mathrm{T}}\mathbf{\Phi}\right)^{-1}\left(\mathbf{\Phi}^{\mathrm{T}}y\right) \tag{4}$$

$$\mathbf{\Phi} = \begin{bmatrix} \varphi_1(l,w)_1 & \cdots & \varphi_{\mathrm{N}}(l,w)_1 \\ \vdots & \ddots & \vdots \\ \varphi_1(l,w)_{\mathrm{M}} & \cdots & \varphi_{\mathrm{N}}(l,w)_{\mathrm{M}} \end{bmatrix} \tag{5}$$

where $b = (\beta_1, \beta_2 \ldots \beta_{\mathrm{n}})$, and M is the number of simulation sample points.

By using the simulation results in Table 1 and combining Eqs. (3) to (5), the proxy model of hysteresis loss factor of the general rotary hinge can be obtained as follows:

$$\begin{aligned}\eta = &-0.10774\text{-}0.12748\Delta r + 0.00275F_g + 0.07342(\Delta r)^2\\ &+ 1.75806\times10^{-4}(\Delta r)F_g - 1.22277\times10^{-5}F_g^2\\ &+ 0.40833(\Delta r)^3\\ &- 8.59694\times10^{-4}(\Delta r)^2F_g + 1.42347\times10^{-7}(\Delta r)F_g^2\\ &+ 2.22867\times10^{-8}F_g^3 - 0.54167(\Delta r)^4\\ &+ 1.66667\times10^{-4}(\Delta r)^3F_g\\ &+ 1.11735\times10^{-6}(\Delta r)^2F_g^2 - 6.66667\times10^{-10}(\Delta r)F_g^3\\ &- 1.45833\times10^{-11}F_g^4\end{aligned} \tag{6}$$

The accuracy must be determined for the obtained approximate polynomial expression. The commonly used determination parameters are deviation *RE*, complex correlation coefficient R^2, root-mean-square error *RMSE* and modified complex correlation coefficient R^2_{adj}.

$$RE = \frac{\tilde{y}_i - y_i}{y_i} \tag{7}$$

$$R^2 = 1 - \frac{SSE}{SST} \tag{8}$$

$$R^2_{\mathrm{adj}} = 1 - \frac{M-1}{M-N}\left(1 - R^2\right) \tag{9}$$

$$RMSE = \left(\frac{SSE}{M-N-1}\right)^{0.5} \tag{10}$$

where y_i is the finite element simulation result;*SSE* is mean square; and *SST* is the sum of the residual mean square.

$$SST = \sum_{i=1}^{M}(y_i - \bar{y})^2 \tag{11}$$

$$SSE = \sum_{i=1}^{M}(y_i - \tilde{y})^2 \tag{12}$$

The value R^2 is between 0 and 1. The closer the value is to 1, the more accurate the approximation of the response equation will be. The approximation degree does not necessarily mean good when the value of R^2 is close to 1. The more variables are in the response equation, the more R^2 tends to increase. Meanwhile, the larger the R^2_{adj} is and the smaller *RE* and *RMSE* are, the better the fitting effect will be.

The relative errors between the finite element simulation and the approximate solution of the proxy model of the loss factor for the general rotary hinge are shown in Table 2. From Eq. (7) to (12), the error determination parameters between the response surface agent model and the finite element simulation results can be calculated as listed in Table 3. The relative error *RE* is no more than 0.855%, and the correlation coefficient R^2 and the modified correlation coefficient R^2_{adj} are both close to 1. Thus, the established agent model has sufficient accuracy. Fig. 6 shows the response surface of the hysteresis loss factor for the general rotary hinge.

TABLE 2. The relative errors of the hysteresis loss factor between simulation value and approximate solution.

Num.	Simulation values η	Approximate solutions	Deviation /%
1	0.0656	0.0658669	0.407
2	0.109	0.1082237	-0.712
3	0.0997	0.1005502	0.853
4	0.0895	0.0890665	-0.484
5	0.0849	0.0849927	0.109
6	0.0554	0.0553094	-0.164
7	0.0989	0.0988767	-0.024
8	0.0918	0.092122	0.351
9	0.0811	0.0808653	-0.289
10	0.0759	0.0759265	0.035
11	0.0466	0.0465159	-0.180
12	0.0901	0.0903449	0.272
13	0.0841	0.0840069	-0.111
14	0.0731	0.072922	-0.244
15	0.0674	0.0675102	0.164
16	0.0401	0.0400865	-0.034
17	0.0831	0.0833282	0.275
18	0.0775	0.0770049	-0.639
19	0.0658	0.0661367	0.512
20	0.0608	0.0607437	-0.093
21	0.0354	0.0353212	-0.223
22	0.0769	0.0772265	0.425
23	0.0712	0.0706159	-0.820
24	0.0596	0.0601094	0.855
25	0.0555	0.0553269	-0.312

TABLE 3. Evaluation of the agent model for the general rotary hinge.

	R^2	R^2_{adj}	RE
η	0.99964	0.99914	(-0.820%)-(0.855%)

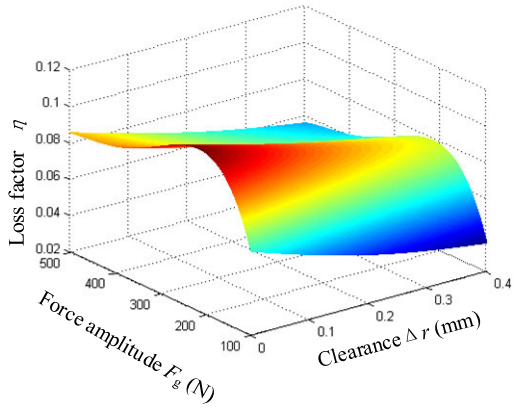

FIGURE 6. Response surface of hysteresis loss factor for the general rotary hinge.

B. PARAMETER STUDIED

According to the response surface of the hysteresis loss factor of the general rotary hinge, the loss factor decreases with the increase of clearance and increases first and then decreases with the increase of force amplitude. For further explanation, Fig. 7 shows the change of loss factor with the hinge clearance when the applied force amplitude is 300 N, Fig. 8 shows the change of loss factor with the applied force amplitude when the hinge clearance is 0.3 mm.

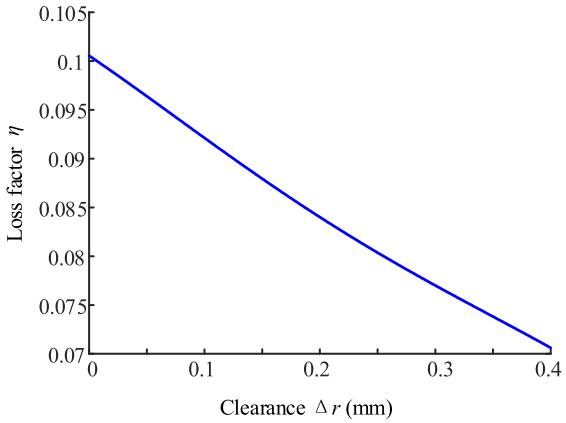

FIGURE 7. Influence of clearance on hysteresis loss factor.

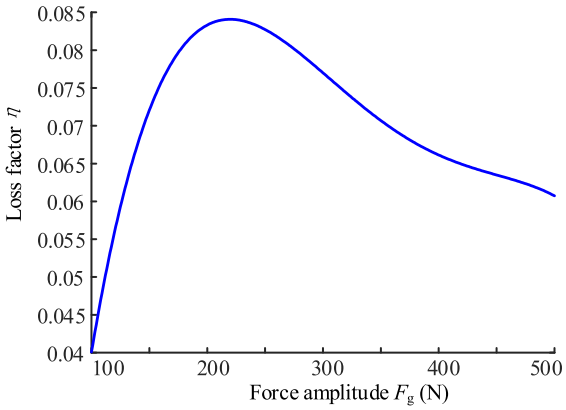

FIGURE 8. Influence of force amplitude on hysteresis loss factor.

The applied force amplitude of the hinge is external load, which is not related to the hinge itself. By contrast, the hinge clearance is the optimal design target of the hinge itself. Increasing the clearance of hinge can effectively reduce the loss factor but will lead to motion errors and other problems, which is contradictory. Increasing hinge clearance means reducing the contact areas. Therefore, angular contact ball bearings can be installed to eliminate the clearance of the hinge through bearing preloading. In this way, only the contact between the ball and the raceway can be retained to eliminate the clearance and reduce the contact area of hinges. Finally, the goal of reducing the hinge's hysteresis loss factor can be achieved.

IV. HYSTERESIS MODEL OF MODIFIED ROTARY HINGE

A. OPTIMIZATION DESIGN

According to the analysis of III-B, the modified hinge is shown in Fig. 8. The clearance was removed by using a

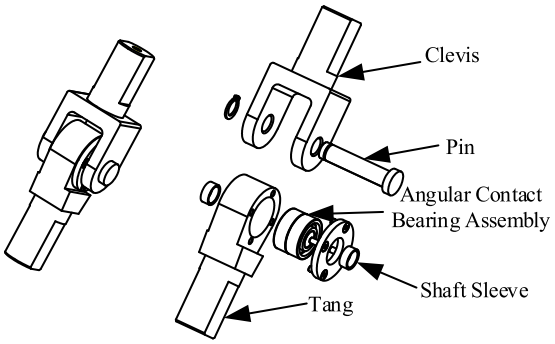

FIGURE 9. Schematic diagram of hinge optimisation design.

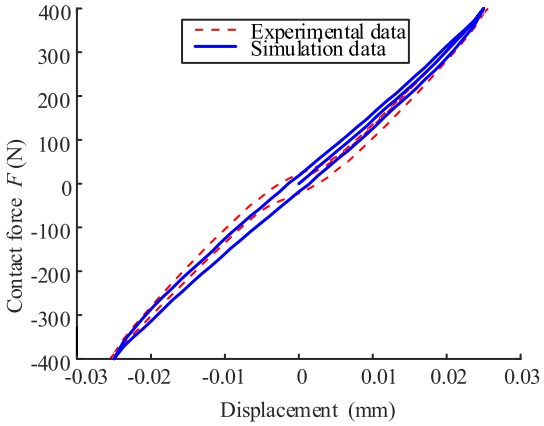

FIGURE 10. Hysteresis test verification of modified rotary hinge.

pair of preloaded angular contact ball bearings. The outer races of the bearing pair were epoxied to the tang. A plate with four screws pinched the outer races together before the epoxy dried, providing the bearing with preload. After liquid nitrogen refrigeration, the pin passed through the inner races and the clevis with epoxy, eliminating the clearance between the tang and outer races, inner races and pin, clevis and pin. In comparison with the general rotary hinge, the modified rotary hinge only retains the contact between the bearing balls and the raceway, eliminating any possibility of clearance. The hysteresis of the modified rotary hinge was then analysed to verify the conjecture.

B. HYSTERESIS ANALYSIS OF MODIFIED ROTARY HINGE

The finite element model of the modified hinge was also established in the finite element software ABAQUS. The tang and clevis were made of aluminum alloy. The material of the pin was 45 steel, and the bearing material was GCr15 with Young's Modulus of 208 GPa and Poisson's Ratio of 0.3. The contacts were defined on the contact surfaces between the outer race and tang, the bearing inner ring and shaft and the shaft and double lug plate, respectively. The tang was fixed and reciprocating force F_g was applied to the clevis. Meanwhile, axial preloading force F_p was applied to the bearing. The other settings of the model were consistent with the finite element model of the general rotary hinge.

To verify the correctness and accuracy of finite element simulation, the hysteresis of the modified rotary hinge was also measured by using the hysteresis measurement platform shown in Fig. 4. The comparison between the test measurement data and the finite element simulation data is shown in Fig. 10. Thus, the test measurement curve and the simulation curve are basically identical in shape. To be specific, under the maximum contact force 400 N and the preloading force 0 N, the contact displacement obtained by simulation was 0.0250 mm. The contact displacement measured by the test was 0.0254 mm and the error was 1.57%. Through calculation, the loss factor of the hinge obtained by finite element simulation was 0.0488, and the loss factor measured by the test was 0.0508, with the error of 3.94%. The error of contact displacement and loss factor are within 5%, and the simulation curve is consistent with the experimental curve. Thus, the finite element simulation model is considered correct and can be used as a method to study the hysteresis of the modified rotary hinge.

Due to multiple contact surfaces, the solution is complex, time consuming and prone to non-convergence for the modified hinge. The response surface method was also adopted for analysis. The finite element simulation was used to calculate the sample points, and the proxy model was established by using quadric polynomials. For the modified hinge, preload F_p and force amplitude F_g were selected as variables. The variation ranges were 0–200 N and 100–500 N, respectively. Twenty-five experimental sample points were obtained as listed in Table 4.

TABLE 4. Simulation data of hysteresis loss factor for the modified rotary hinge.

Num.	F_p /mm	F_g/ N	η	Num.	F_p /mm	F_g/N	η
1	0	100	0.0161	14	100	400	0.0568
2	0	200	0.0721	15	100	500	0.0483
3	0	300	0.0641	16	150	100	0.0252
4	0	400	0.0481	17	150	200	0.0882
5	0	500	0.0411	18	150	300	0.0763
6	50	100	0.0191	19	150	400	0.0592
7	50	200	0.0775	20	150	500	0.0506
8	50	300	0.0688	21	200	100	0.0271
9	50	400	0.0528	22	200	200	0.0921
10	50	500	0.0454	23	200	300	0.0789
11	100	100	0.0222	24	200	400	0.0613
12	100	200	0.0832	25	200	500	0.0525
13	100	300	0.0731				

By using the simulation results in Table 4 and combining Eqs. (3) and (5), the proxy model of hysteresis loss factor for the modified rotary hinge can be obtained as follows:

$$\begin{aligned}\eta = &-0.21797\text{-}1.06155 \times 10^{-4}F_p + 3.72353 \times 10^{-3}F_g \\ &+ 6.24476 \times 10^{-7}F_p^2 + 2.03960 \times 10^{-6}F_pF_g \\ &- 1.67340 \times 10^{-5}F_g^2\end{aligned}$$

TABLE 5. The relative errors of the hysteresis loss factor between simulation value and approximate solution.

Num.	Simulation values η	Approximate solutions η	Deviation /%
1	0.0161	0.016032	-0.422
2	0.0721	0.0726127	0.711
3	0.0641	0.0631197	-1.529
4	0.0481	0.048823	1.503
5	0.0411	0.0409126	-0.456
6	0.0191	0.018862	-1.246
7	0.0775	0.0779547	0.587
8	0.0688	0.0683642	-0.633
9	0.0528	0.0531455	0.654
10	0.0454	0.0452737	-0.278
11	0.0222	0.022274	0.333
12	0.0832	0.0832613	0.073
13	0.0731	0.0730723	-0.038
14	0.0568	0.056547	-0.445
15	0.0483	0.0484454	0.301
16	0.0252	0.025248	0.190
17	0.0882	0.0878227	-0.428
18	0.0763	0.0768442	0.713
19	0.0592	0.0589375	-0.443
20	0.0506	0.0506477	0.094
21	0.0271	0.027284	0.679
22	0.0921	0.0914487	-0.707
23	0.0789	0.0797997	1.140
24	0.0613	0.060747	-0.902
25	0.0525	0.0526206	0.230

$$
\begin{aligned}
&- 2.81333 \times 10^{-9} F_p^3 - 2.20367 \times 10^{-9} F_p^2 F_g \\
&- 6.23765 \times 10^{-9} F_p F_g^2 \\
&+ 3.10783 \times 10^{-8} F_g^3 + 3.46667 \times 10^{-12} F_p^4 \\
&+ 4.13333 \times 10^{-12} F_p^3 F_g \\
&+ 1.16327 \times 10^{-12} F_p^2 F_g^2 + 5.95 \times 10^{-12} F_p F_g^3 \\
&- 2.08667 \times 10^{-11} F_g^4
\end{aligned} \tag{13}
$$

The relative errors of the hysteresis loss factor between the finite element simulation and the approximate solution of the proxy model for modified hinge are shown in Table 5. From equations (7) to (12), the error determination parameters between the response surface agent model and the finite element simulation results can be calculated, as shown in Table 6. The relative error RE was no more than 1.529%. The correlation coefficient R^2 and the modified correlation coefficient R^2_{adj} were close to 1. Hence, the established agent model has sufficient accuracy. Figure 11 shows the response surface of the hysteresis loss factor of the modified rotary hinge.

TABLE 6. Evaluation of the agent model for modified rotary hinge.

	R^2	R^2_{adj}	RE
η	0.99961	0.99906	-1.529%~1.503%

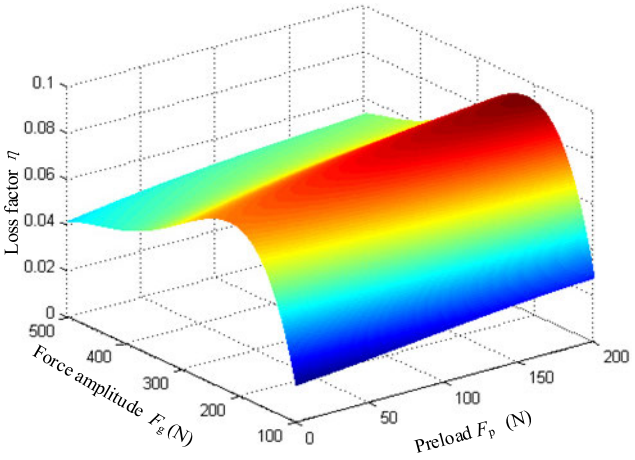

FIGURE 11. Response surface of hysteresis loss factor for the modified rotary hinge.

The response surface of the hysteresis loss factor of the modified rotary hinge indicates that the loss factor increases with the increase of preload and increases first and then decreases with the increase of force amplitude. Specifically, Fig. 12 shows the change of loss factor with the preload when the applied force amplitude is 200 N. Fig. 13 shows the change of loss factor with the applied force amplitude when the preload is 100 N.

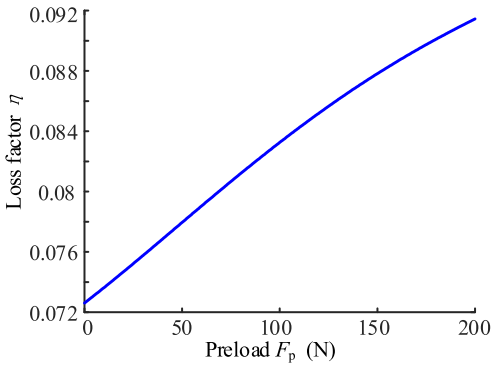

FIGURE 12. The influence of preload on hysteresis loss factor.

V. ANALYSIS AND VERIFICATION OF HYSTERESIS

A. ANALYSIS OF HINGE HYSTERESIS

The comparison diagram of the response surface between the general rotary hinge and the modified rotary hinge is shown in Fig. 14. A shaded part is a plane with the hysteresis loss factor of 0.05, which divides the response surface of the general rotary hinge into regions a)-1 and a)-2, and the response surface of the modified rotary hinge into regions b)-1, b)-2 and

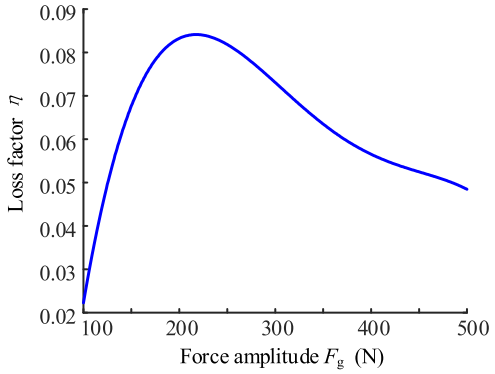

FIGURE 13. The influence of force amplitude on the hysteresis loss factor.

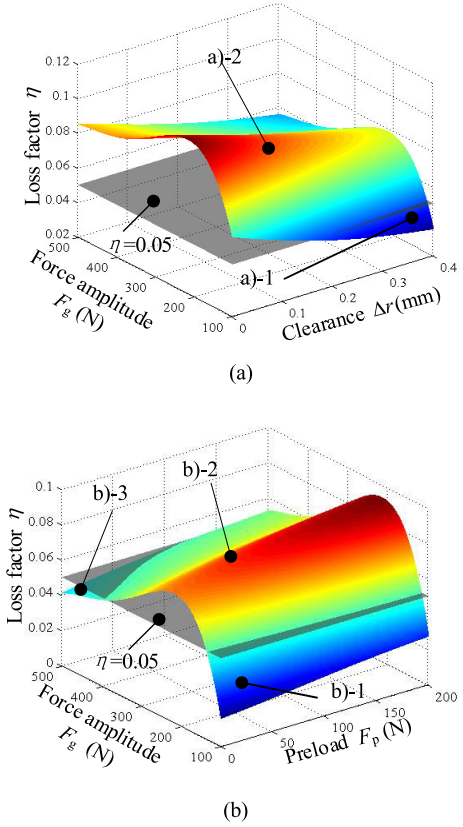

FIGURE 14. Comparison diagram of response surfaces. (a) Response surface of the general rotary hinge. (b) Response surface of the modified rotary hinge.

b)-3, respectively. Assuming that the hysteresis loss factor had to be reduced to less than 0.05, only the area a)-1 met the requirement for general rotary hinges. The clearance of the hinge in this area should be greater than 0.2248 mm, which was not allowed for a high-precision mechanism. By contrast, for the modified rotary hinge, the regions b)-1 and b)-3 met the requirement. As for the region b)-1, only a relatively small force amplitude of the hinge was required to meet the requirement of hysteresis loss factor. As for the region b)-3, a large force amplitude and a small preload force of the hinge were required to meet the requirement. The two cases were easy to implement.

Moreover, when the ranges of force amplitude, clearance of rotary hinge and preload were 100–500 N, 0–0.4 mm and 0–200 N, respectively. The minimum and maximum hysteresis loss factors of general rotary hinge were 0.0353 and 0.1087, whereas the modified rotary hinges were 0.0160 and 0.0733, reducing by 54.67% and 32.57%, respectively.

As indicated in Fig. 14, when the hysteresis loss factor was lower than a certain value, the modified hinge satisfied a larger area than the general rotary hinge. In addition,, under the same force amplitude, the hysteresis loss factor of the general rotary hinge could be reduced by increasing the clearance, which was unpractical. However, the hysteresis loss factor of the modified rotary hinge could be reduced by reducing the preload, which was practical. Therefore, the hysteresis loss factor of the modified hinge was low and suitable for engineering applications.

B. EXPERIMENTAL VERIFICATION

To further confirm the relationship between the repeatability and the hysteresis loss factor of the hinge, as shown in Fig. 15, the experimental measuring platform of the repeatability of the hinge was set up. The clevis of the hinge was fixed. In addition, the tang was connected to the pendulum, and weight was applied as the radial load of the hinge. The KEYENCE LK-G5001 high-precision laser displacement sensor with a resolution of 0.1 μm was installed on the swing side of the hinge to measure the position l at the distance L from the rotation centre of the hinge.

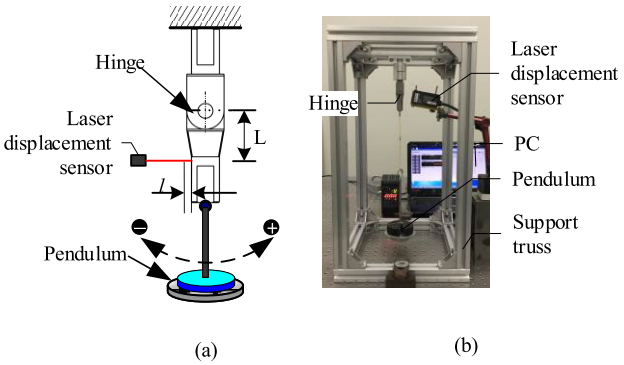

FIGURE 15. Experimental measuring platform of repeatability. (a) Schematic diagram. (b) Experiment device.

When measuring, add weight 100 N into the single pendulum at first, adjust the indicator of laser displacement sensor to zero when the single pendulum is stationary, then make the single pendulum swing. When the single pendulum is stationary again, record the reading of the display, which is the position l of hinge deviating from the vertical direction. Then, put the single pendulum at the same height to make it continue to swing. Record the reading after the pendulum is stationary. Repeat the above process to obtain the position l.

A total of 200 measurements of the general rotary hinge and modified rotary hinge were carried out respectively. The measurement results were approximated as a normal distribution. As shown in Fig. 16, the column bar was the number of sample distributions, and the lines were the approximately equivalent normal distribution curves. The mean value μ and standard deviation σ of the normal distribution were obtained. The measure falls within the confidence interval $(\mu-3\sigma, \mu+3\sigma)$ with a confidence coefficient of 99.74%, according to the PauTa criterion (3σ criterion). It is feasible to consider 6σ, the size of the interval, as the size of the position error. For the general and modified rotary hinges, the standard deviations were obtained as 1.0942 μm and 0.2388 μm, respectively.

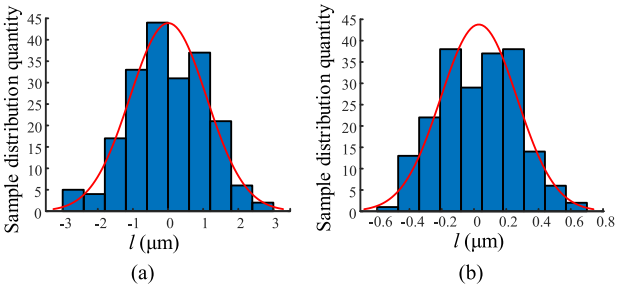

FIGURE 16. Measurement results of position errors. (a) General rotary hinge. (b) Modified rotary hinge.

Here, the error of the hinge's turning angle is regarded as the repeatability of the hinge. Because the position error 6σ is small, as indicated in Fig. 13, the repeatability of the hinge can be expressed as Eq. (14).

$$\theta = \frac{\arcsin(6\sigma/L)}{180}\pi \tag{14}$$

where $L = 25$ mm.

Also, the hysteresis loss factors can be calculated by substituting the parameters of the hinges into Eqs. (6) and (13). The experimental repeatability of the two type hinges can be calculated by Eq. (14). The correlation between repeatability and hysteresis loss factor was shown in Table 7, compared with the general rotary hinge. The hysteresis loss factor of the modified rotary hinge was 75.72% lower, and the repeatability was 78.19% higher. This illustrated that by reducing the hysteresis loss factor, the repeatability of the hinge can be improved effectively.

TABLE 7. Correlation between repeatability and hysteresis loss factor.

	η	θ / rad
General hinge	0.0659	2.6260×10^{-4}
Modified hinge	0.0160	5.7312×10^{-5}
The change	75.72%	78.18%

VI. CONCLUSION

The hysteresis of a hinge is difficult to eliminate and control and significantly impacts the precision of the mechanism. By far, the majority of studies are based on the equivalent model, thus lacking experimental verification and far from the actual situation. In this paper, ABAQUS/Standard 6.14-4 software was employed to analyse the contact deformation. The model of the general rotary hinge's hysteresis was established by combining the FEM with the experimental verification. The response surface of the hysteresis loss factor was established by the RSM. Results show that the hinge was optimised. By comparing the response surfaces of the two types of hinges, the modified hinge can effectively reduce the hysteresis loss factor. Furthermore, the experimental measuring platform of the repeatability of the hinge was set up to confirm the relationship between the hinge repeatability and the hysteresis loss factor. Experimental results showed that, in comparison with the general rotary hinge, the loss factor of the modified rotary hinge was reduced by 75.72%, and the repeatability of the modified hinge was increased by 78.19%. The repeatability of the hinge can be effectively improved by reducing the hysteresis loss factor.

By using this method, the model of the hinge's hysteresis loss factor can be established accurately. The hysteresis loss factor can be reduced through optimal design to improve the repeatability of the hinge. Moreover, according to the response surface of the hinge, the external load, clearance and preload can be selected reasonably to reduce the hysteresis loss factor and improve repeatability. This method can provide reference and guidance for the hinge design of the high-precision mechanism.

REFERENCES

[1] V. Hassani, T. Tjahjowidodo, and T. N. Do, "A survey on hysteresis modeling, identification and control," *Mech. Syst. Signal Process.*, vol. 49, nos. 1–2, pp. 209–233, 2014.

[2] M. Lake, P. Warren, L. Peterson, "A revolute joint with linear load-displacement response for precision deployable structures," in *Proc. 37th Struct., Structural Dyn. Mater. Conf.*, 1996, p. 1500.

[3] M. S. Lake, P. A. Warren, and L. D. Peterson, "A revolute joint with linear load-displacement response for a deployable lidar telescope," in *Proc. 30th Aerosp. Mech. Conf. Symp.*, Hampton, VA, USA, May 1996.

[4] M. Lake, J. Fung, K. Gloss, D. Liechty, D. Liechty, M. Lake, J. Fung, and K. Gloss, "Experimental characterization of hysteresis in a revolute joint for precision deployable structures," in *Proc. 38th Struct., Struct. Dyn., Mater. Conf.*, Apr. 1997, p. 1379.

[5] M. S. Lake and M. R. Hachkowski, "Design of mechanisms for deployable, optical instruments: Guidelines for reducing hysteresis," NASA, Washington, DC, USA, Tech. Rep. NASA TM-2000-210089, Mar. 2000.

[6] M. Lake and M. Hachkowski, "Mechanism design principles for optical-precision, deployable instruments," in *Proc. 41st Struct., Struct. Dyn., Mater. Conf. Exhibit*, Apr. 2000, p. 1409.

[7] S. J. Bullock, "Identification of the nonlinear micronlevel mechanics of joints for deployable precision space structures," Tech. Rep. CU-CAS-96-13, 1997.

[8] S. Bullock and L. Peterson, "Nonlinear micron-level mechanics of a precision deployable space structure joint," in *Proc. 37th Struct., Struct. Dyn. Mater. Conf.*, Apr. 1996, p. 1333.

[9] P. A. Warren and L. D. Peterson, "Sub-micron nonlinear shape mechanics of precision deployable structures," Ph.D. dissertation, Dept. Aerosp. Eng. Sci., Univ. Colorado, Boulder, CO, USA, 1996.

[10] J. D. Hinkle, "Frictional microslip due to roughness in metallic interfaces at the nanometer scale," Tech. Rep. CU-CAS-98-12, May 1999.

[11] M. R. Hachkowski, "Reduction of hysteresis in the load-displacement response of precision deployment mechanisms through load path management," Tech. Rep. CU-CAS-98-07, May 1999.

[12] L. M. R. Hardaway, "Stability and mechanics of precision deployable structures under nanometer deformation," Tech. Rep. CU-CAS-00-12, May 2000.
[13] J. C. Heald, "Deployment repeatability in mechanically jointed precision structures," Tech. Rep. CU-CAS-03-06, 2004.
[14] J. N. Footdale, "Multi-axis real-time hybrid testing for precision aerospace structures," Ph.D. dissertation, Dept. Aerosp. Eng., Univ. Colorado, Boulder, CO, USA, 2008.
[15] S. K. Jeon, "Characterization of Hertzian rolling microslip in precision revolute joints for deployable space structures," Ph.D. dissertation, Dept. Aerosp. Eng. Sci., Univ. Colorado, Boulder, CO, USA, 2009.
[16] T. Mann, "Precision joint modeling for quasi-static and dynamic response," Ph.D. dissertation, Dept. Aerosp. Eng., Univ. Colorado, Boulder, CO, USA, 2009.
[17] O. R. Stohlman, "Repeatability of joint-dominated deployable masts," Ph.D. dissertation, Dept. Mech. Eng., California Inst. Technol., Pasadena, CA, USA, 2011.
[18] K. Worden and G. Manson, "On the identification of hysteretic systems. Part I: Fitness landscapes and evolutionary identification," *Mech. Syst. Signal Process.*, vol. 29, pp. 201–212, May 2012.
[19] K. Worden and W. E. Becker, "On the identification of hysteretic systems. Part II: Bayesian sensitivity analysis and parameter confidence," *Mech. Syst. Signal Process.*, vol. 29, pp. 213–227, May 2012.
[20] M. Ruderman and T. Bertram, "Modeling and observation of hysteresis lost motion in elastic robot joints," *IFAC Proc. Volumes*, vol. 45, no. 22, pp. 13–18, 2012.
[21] J. Swevers, F. Al-Bender, C. G. Ganseman, and T. Projogo, "An integrated friction model structure with improved presliding behavior for accurate friction compensation," *IEEE Trans. Autom. Control*, vol. 45, no. 4, pp. 675–686, Apr. 2000.
[22] T. Misaka, J. Herwan, O. Ryabov, S. Kano, H. Sawada, N. Kasashima, and Y. Furukawa, "Prediction of surface roughness in CNC turning by model-assisted response surface method," *Precis. Eng.*, vol. 62, pp. 196–203, Mar. 2020.
[23] H. Yang, L. Liu, H. Guo, F. Lu, and Y. Liu, "Wrapping dynamic analysis and optimization of deployable composite triangular rollable and collapsible booms," *Struct. Multidisciplinary Optim.*, vol. 59, no. 4, pp. 1371–1383, Apr. 2019.
[24] H. Yang, Z. Deng, R. Liu, Y. Wang, and H. Guo, "Optimizing the qusai-static folding and deploying of thin-walled tube flexure hinges with double slots," *Chin. J. Mech. Eng.*, vol. 27, no. 2, pp. 279–286, Mar. 2014.

MINGXING GAO received the B.S. and M.S. degrees in mechanical engineering from the School of Mechatronics Engineering, Harbin Institute of Technology, Harbin, China, in 2014 and 2016, respectively, where he is currently pursuing the Ph.D. degree in mechanical engineering. His research interests are design and stability analysis of space deployable and foldable mast.

HONGWEI GUO received the B.S., M.S., and Ph.D. degrees in mechanical engineering from the School of Mechatronics Engineering, Harbin Institute of Technology, Harbin, China, in 2003, 2005, and 2009, respectively. He is currently a Professor and a Doctoral Supervisor with the State Key Laboratory of Robotics and Systems, Harbin Institute of Technology, Harbin. His research interests include the innovative design of the configuration of deployable mechanism, aircraft bionic intelligent deformed wing, and space deployable mast.

RONGQIANG LIU received the B.S. degree in mechanical engineering from the Shandong University of Science and Technology, Tai'an City, China, in 1986, and the M.S. and Ph.D. degrees in mechanical engineering from the School of Mechatronics Engineering, Harbin Institute of Technology, Harbin, China, in 1989 and 1995, respectively. He is currently a Professor and a Doctoral Supervisor with the State Key Laboratory of Robotics and Systems, Harbin Institute of Technology, Harbin. His research interests include the space large deployable mechanism and control, large-aperture deployable antenna mechanism, and landing buffer.

ZONGQUAN DENG received the B.S. and M.S. degrees in mechanical engineering from the School of Mechatronics Engineering, Harbin Institute of Technology, Harbin, China, in 1982 and 1984, respectively. He is currently an Academician of the Chinese Academy of Engineering, a Vice-Chancellor of the Harbin Institute of Technology, a Professor with the State Key Laboratory of Robotics and Systems, Harbin Institute of Technology, Harbin, China. His research interests include the mechanical design theory and related technology of space deployable and foldable mechanism, and special robot.